

2015 International Congress on Ultrasonics, 2015 ICU Metz

## Attenuation Coefficient Estimation of the Healthy Human Thyroid In Vivo

J. Rouyer<sup>a\*</sup>, T. Cueva<sup>a</sup>, A. Portal<sup>b</sup>, T. Yamamoto<sup>b</sup> and R. Lavarello<sup>a</sup>

<sup>a</sup>Laboratorio de Imágenes Médicas, Pontificia Univ. Católica del Perú, Av. Universitaria 1801 - San Miguel, Lima 32, Lima, Perú

<sup>b</sup>Dep. de Radiología, Clínica Centenario Peruano Japonesa, Av. Paso de Los Andes 675 - Pueblo Libre, Lima 32, Lima, Perú

---

Previous studies have demonstrated that attenuation coefficients can be useful towards characterizing thyroid tissues. In this work, ultrasonic attenuation coefficients were estimated from healthy human thyroids *in vivo* using a clinical scanner. The selected subjects were five young, healthy volunteers (age:  $26 \pm 6$  years old, gender: three females, two males) with no reported history of thyroid diseases, no palpable thyroid nodules, no smoking habits, and body mass index less than  $30 \text{ kg/m}^2$ . Echographic examinations were conducted by a trained sonographer using a SonixTouch system (Ultrasonix Medical Corporation, Richmond, BC) equipped with an L14-5 linear transducer array (nominal center frequency of 10 MHz, transducer footprint of 3.8 cm). Radiofrequency data corresponding to the collected echographic images in both transverse and longitudinal views were digitized at a sampling rate of 40 MHz and processed with Matlab codes (MathWorks, Natick, MA) to estimate attenuation coefficients using the spectral log difference method. The estimation was performed using an analysis bandwidth spanning from 4.0 to 9.0 MHz. The average value of the estimated ultrasonic attenuation coefficients was equal to  $1.34 \pm 0.15 \text{ dB/(cm.MHz)}$ . The standard deviation of the estimated average attenuation coefficient across different volunteers suggests a non-negligible inter-subject variability in the ultrasonic attenuation coefficient of the human thyroid.

© 2015 The Authors. Published by Elsevier B.V. This is an open access article under the CC BY-NC-ND license (<http://creativecommons.org/licenses/by-nc-nd/4.0/>).

Peer-review under responsibility of the Scientific Committee of ICU 2015

*Keywords:* Attenuation coefficient; thyroid; quantitative estimation; *in vivo*

---

### 1. Introduction

The thyroid gland is a readily accessible for ultrasound inspection thanks to an easily identifiable location (i.e., below the Adam's apple surrounding the trachea) at a shallow depth (i.e., from 1 to 3 cm). The thyroid cancer is the

---

\* E-mail address: [jrouyer@pucp.pe](mailto:jrouyer@pucp.pe)

most rapidly increasing cancer with a rate of 6% in a period ranging from 2006 to 2010 in the United States of America (American Cancer Society 2014). Ultrasonic B-mode imaging is widely used as a medical tool for assessing the malignancy of thyroid nodules but currently no ultrasonic marker allows the reliable distinction between benign and malignant nodules for all nodules (Frates et al. 2006). As a result, fine-needle aspiration remains the gold standard for thyroid cancer assessment (Amrikachi et al. 2001). Therefore, there is a need to develop non-invasive tools that aid in the identification of malignant tissues in this gland.

Quantitative ultrasound (QUS) parameters have demonstrated potentially useful diagnostic capabilities for thyroid cancer in studies involving small animal models (Lavarello et al. 2013a; Montero et al. 2014; Zenteno et al. 2013; Lavarello et al. 2013b). The estimation of attenuation coefficient slopes allowed differentiating between benign and malignant tissues. Derived parameters from the backscatter coefficient estimates (i.e., effective scatter diameter and effective acoustic concentration) also exhibited interesting differentiation capabilities which were correlated with histological slices. However, the backscatter coefficient estimation requires knowledge of the attenuation coefficient in order to perform frequency-dependent attenuation compensation (Oelze and O'Brien 2002). Therefore, the attenuation coefficient slope is a key parameter in order to perform accurate quantitative tissue characterization.

As a first step towards determining the usefulness of spectral-based quantitative ultrasound for thyroid cancer diagnosis, this study deals with the estimation of the attenuation coefficient slope in healthy human thyroids *in vivo*. Radio-frequency data from five young volunteers were acquired by a trained radiologist using a clinical scanner equipped with a 10 MHz linear array. The spectral log difference method was used for obtaining several estimates of the attenuation coefficient slope. Both intra- and inter-subject variability were calculated and the results were compared to the few studies on attenuation estimation in the thyroid available in the literature.

## 2. Materials and Methods

### 2.1. Attenuation estimation technique

The spectral log difference technique was employed for the estimation of the attenuation coefficient slope. This technique gives accurate attenuation estimates in regions of interest (ROIs) with homogeneous scatter sizes (Labyed and Bigelow 2011). The estimation is based on a spectral comparison between proximal ( $p$ ) and distal ( $d$ ) sub-regions within the ROI. A reference phantom is employed to correct for the diffraction effects and the apparatus transfer function. If the selected region is homogeneous with respect to the scattering sources, then the difference of the logarithm of the spectral ratio in the proximal and distal sub-regions is proportional to the unknown attenuation coefficient, i.e.,

$$\ln \left[ \frac{\langle |S_T(f, z_d)|^2 \rangle}{\langle |S_R(f, z_d)|^2 \rangle} \right] - \ln \left[ \frac{\langle |S_T(f, z_p)|^2 \rangle}{\langle |S_R(f, z_p)|^2 \rangle} \right] + 4(z_p - z_d)\alpha_R(f) = 4(z_p - z_d)\alpha_0 f + c, \quad (1)$$

where  $\langle |S_T|^2 \rangle$  and  $\langle |S_R|^2 \rangle$  are the average power spectra corresponding to the tissue and the reference phantom, respectively,  $f$  is the frequency,  $z_p$  and  $z_d$  are the depth of the proximal and distal sub-ROIs,  $c$  is a numerical constant, and  $\alpha_R(f)$  is the attenuation function of the reference phantom. The attenuation function of the thyroid was considered linear with frequency within the analysis frequency range of this study, and defined as  $\alpha_0 f$  with  $\alpha_0$  the attenuation coefficient slope of the thyroid. The estimates of the attenuation coefficient slope ( $\hat{\alpha}_0$ ) were obtained using least absolute deviation regression.

### 2.2. Data acquisition and estimation procedure

The experimental protocol was approved by the Ethics Committee of the Pontificia Universidad Católica del Perú. Briefly, the selected subjects were five young, healthy volunteers (age: 26 +/- 6 years old, gender: three females, two males) with no reported personal or family history of thyroid diseases, no palpable thyroid nodules, no

smoking habits, and body mass index less than  $30 \text{ kg/m}^2$ . Echographic examinations were conducted by a trained sonographer using a SonixTouch system (Ultrasonix Medical Corporation, Richmond, BC) equipped with an L14-5 linear transducer array (nominal center frequency of 10 MHz, transducer footprint of 3.8 cm). Rf-data corresponding to the collected echographic images were digitized at a sampling rate of 40 MHz. Several frames of the thyroid images were acquired in the longitudinal view (i.e. along the trachea) as this orientation enables to inspect a larger part of the gland. The attenuation coefficient slope estimates were obtained using an analysis frequency band ranging from 4 to 9 MHz.

The reference phantom consisted in an agar-based matrix with embedded glass beads uniformly arranged with a diameter ranged between 90 and 106 microns and a scatter density of 3.5 scatterers per  $\text{mm}^3$ . The attenuation coefficient slope and speed of sound in the reference phantom were 0.68 dB/(cm.MHz) and 1540 m/s, respectively. The reference phantom acquisitions were performed using the exact same system settings used for scanning the thyroids.

The attenuation coefficient slope estimates were calculated in a rectangular domain. Particular attention was paid to select thyroid tissues with apparent speckle homogeneity. The lateral ROI size was chosen equal to 0.56 cm (i.e., about 20 wavelengths at the center frequency of the analysis band) which corresponded to 48 rf-lines in the image. The ROIs had a 50% overlap ratio in the lateral direction. The axial ROI dimension was set as a variable parameter which depended on the size and morphology of each studied thyroid gland. The axial sub-ROIs (i.e., proximal and distal) had a fixed dimension equal to  $L = 0.35 \text{ cm}$  (i.e., about 14 wavelengths at the center frequency of the analysis band) in order for the expression in (1) to be valid (i.e.,  $\alpha(f)L < 0.5$ , see (Oelze and O'Brien 2002)). Four different frames for each one of the five volunteers were used in the estimation process.

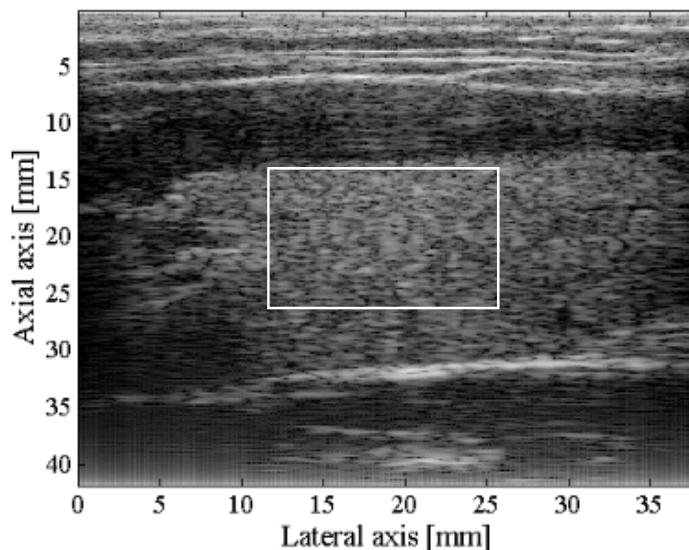


Fig. 1. B-mode image of the right thyroid lobe of volunteer #1 (longitudinal view). The white square depicts the usable domain of thyroid tissue. This domain was segmented into several ROIs along the lateral direction.

### 3. Results and Discussion

A sample longitudinal B-mode image of a thyroid is shown in Fig. 1. The employed analysis region is depicted by a white square, which was segmented into several ROIs as indicated in the previous section. Figure 2(a) shows the typical averaged power spectra ( $\langle |S|^2 \rangle$ ) of the proximal and distal sub-ROIs in the case of the thyroid tissue and the reference phantom. Within the selected bandwidth, the frequency content of the distal rf-signals are lower

than the proximal sub-ROI and clearly shows the loss of the high frequency content with increasing depth. The left term of (1), which corresponds to the spectral log difference compensated by the attenuation of the reference phantom, is plotted in Fig. 2(b). The coherent component of the backscattered spectra introduces an oscillatory noise in this function. The use of an L1-linear regression was selected in order to reduce the effects of outliers in the attenuation slope estimation process.

Table 1. The average estimates ( $\langle \widehat{\alpha}_0 \rangle$ ) and the standard deviation of the estimates ( $\sigma_{\widehat{\alpha}_0}$ ) for all five volunteers in this study. Some relevant parameters employed for the estimation of the attenuation coefficient slopes, including the average number of ROIs per frame (ROI/frame), the total number of ROIs (ROI total), and the average distance between the center of the proximal and distal sub-ROIs ( $\langle |z_p - z_d| \rangle$ ), are also listed.

Volunteer #	ROI/frame	ROI total	$\langle  z_p - z_d  \rangle$ [cm]	$\langle \widehat{\alpha}_0 \rangle$ [dB/(cm.MHz)]	$\sigma_{\widehat{\alpha}_0}$ [dB/(cm.MHz)]
1	6	29	1.18	1.23	0.17
2	8.25	33	0.46	1.40	0.39
3	9.5	46	0.49	1.19	0.34
4	5	20	0.77	1.57	0.46
5	5	20	1.31	1.33	0.11

The estimates of the attenuation coefficient slope of the thyroids are presented in Table 1. This table also includes some relevant parameters which were used in the estimation process. The total number of attenuation coefficient slope estimates per volunteer depended on the size of the usable thyroid area in each image. Overall, the average attenuation coefficient slope considering all five volunteers was  $1.34 \pm 0.15$  dB/(cm.MHz).

To our knowledge, there is one study in the literature dealing with the attenuation estimation in human thyroids in vivo (Fujii et al. 2003). In this study, the attenuation coefficient slope for normal thyroids was estimated to be  $1.50 \pm 0.26$  dB/(cm.MHz). The estimates of attenuation coefficient slope presented in the current study are in close agreement with the values in (Fujii et al. 2003), which were obtained using a modified version of the spectral shift central frequency method (Fujii et al. 2002), and using a wide age range (10 to 76 years old). Therefore, these results suggest attenuation coefficient slope estimation from thyroids in vivo can be reliably performed using spectral-based methods with pulse-echo data.

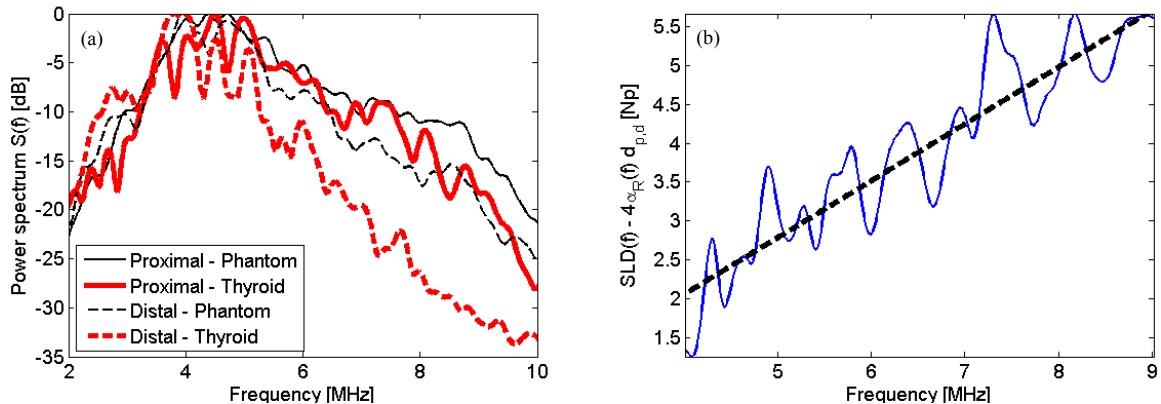


Fig. 2. Example of the calculation for one typical ROI. (a) The averaged power spectra of the thyroid tissue in thick red lines and the reference phantom in thin black lines. Proximal and distal sub-ROIs curves are plotted in plain and dashed line, respectively. (b) The left term of (1) is plotted with the corresponding L1-linear regression, respectively in plain blue line and in dashed black line.

The mean values for each volunteers are spread between 1.19 and 1.57 dB/(cm.MHz), which suggests a non-negligible inter-subject variability. This variability may be partially due to limitations of the estimation algorithm, but may also be due to variations in the actual attenuation coefficients across subjects even though the volunteers were in a narrow age range. The employed technique was able to estimate the attenuation coefficient slope with a relatively low intra-subject variation (between 8 % and 30 %), which suggests that the attenuation coefficient can be reliably estimated in a clinical context.

## Acknowledgment

This work was supported by CONCYTEC grant 8-2013-FONDECYT.

## References

- American Cancer Society, 2014. "Cancer Facts & Figures."
- M. Amrikachi., I. Ramzy, S. Rubinfeld, and T. M. Wheeler, 2001. "Accuracy of Fine-Needle Aspiration of Thyroid." *Archives of pathology & laboratory medicine* 125(4):484–88.
- M. C. Frates, et al., 2006. "Management of Thyroid Nodules Detected at US: Society of Radiologists in Ultrasound Consensus Conference Statement." *Ultrasound Quarterly* 22(4):231–38.
- Y. Fujii et al. 2002. "A New Method for Attenuation Coefficient Measurement in the Liver." *Journal of Ultrasound in Medecine* 21:783–88.
- Y. Fujii N. Taniguchi, N. Itoh, and K. Omoto, 2003. "Attenuation Coefficient Measurement in the Thyroid." *Journal of Ultrasound in Medicine* 22(10):1067–73.
- Y. Labyed and T. Bigelow, 2011. "A Theoretical Comparison of Attenuation Measurement Techniques from Backscattered Ultrasound Echoes." *The Journal of the Acoustical Society of America* 129(4):2316–24.
- R. Lavarello, W. B. Ridgway, S. Sarwate and M. L. Oelze, 2013. "Imaging of Follicular Variant Papillary Thyroid Carcinoma in a Rodent Model Using Spectral-Based Quantitative Ultrasound Techniques.", *IEEE 10th International Symposium on Biomedical Imaging (ISBI)*, 732–35.
- R. Lavarello, W. B. Ridgway, S. Sarwate, and M. L. Oelze, 2013. "Characterization of Thyroid Cancer in Mouse Models Using High-Frequency Quantitative Ultrasound Techniques." *Ultrasound in Medicine & Biology* 39(12):2333–41.
- M. L. Montero, O. Zenteno, B. Castaneda, M. L. Oelze, and R. Lavarello, 2014. "Evaluation of Classification Strategies Using Quantitative Ultrasound Markers and a Thyroid Cancer Rodent Model." *IEEE International Ultrasonics Symposium (IUS)*, 1916–19.
- M. L. Oelze and. W. D. O'Brien, 2002. "Frequency-Dependent Attenuation-Compensation Functions for Ultrasonic Signals Backscattered from Random Media." *The Journal of the Acoustical Society of America* 111(5):2308.
- O. Zenteno, W. B. Ridgway, S. Sarwate, M. L. Oelze, and R. Lavarello, 2013. "Ultrasonic Attenuation Imaging in a Rodent Thyroid Cancer Model." *IEEE International Ultrasonics Symposium (IUS)* 88–91.